A STUDY OF SHORT-PERIOD MICROSEISMS

by

Leland Timothy Long

A thesis submitted in partial fulfillment of
the requirements for the degree of
MASTER OF SCIENCE IN GEOPHYSICS

NEW MEXICO INSTITUTE OF MINING AND TECHNOLOGY

June 1964

Abstract

The sources, directions of arrival, frequencies, velocities, and particle motions of microseisms in the frequency range of 2 to 5 cps near Socorro, New Mexico, are described. Sources of short-period microseisms include vehicular traffic, construction equipment and trains. Trains passing north-south through the Rio Grande valley at a mean distance of 3 miles from the recording equipment produced the strongest microseisms. The directions to the trains could be successfully determined from the microseisms in the zone between N-50-E and S-70-E. Outside this zone the increased topographic relief seriously attenuates and scatters the train microseisms.

Peaks in the number of determinations of frequency occurred near 2.9 and 3.4 cps. The interaction of surface waves of these two frequencies produces a beat effect found often of the records of the train microseisms.

The measured phase velocities of the train microseisms ranged from 1050 to 2200 ft/sec. A peak in the distribution of velocity measurements occurred at 1350 ft/sec, a velocity very near the measured phase velocities of 2.9 cps Rayleigh waves. Particle motions were generally complex combinations of Love and Rayleigh

waves. Isolated Rayleigh wave components showed a tilt of the major axis toward the direction of propagation and a mean axial ratio of 0.58.

Table of Contents

List of Figures

Figure Page

A STUDY OF SHORT-PERIOD MICROSEISMS

Introduction

Microseisms are oscillations of the ground with periods that range over the entire measurable spectrum of ground motion. They exhibit neither sharp beginnings nor abrupt endings, but appear to be a continuous sequence of short wave-trains with randomly assorted frequencies and amplitudes. They can be detected by all seismographs having sufficient magnification at any time. Their amplitudes vary with the proximity and nature of the generating source and with the path over which they travel.

Microseisms are generated both by nature (atmospheric disturbances) and man (industrial activity). The ultimate source of most natural microseismic activity is in atmospheric disturbances. All theories on the origin of natural microseisms may be considered as attempts to explain how a significant transfer of energy can take place from the air to solid surface materials (Haskell, 1951). Industrial activity such as construction work, traffic, heavy industrial machines, and trains transfer energy directly into the ground in the form of microseisms. Close to the source, industrial microseisms exhibit much greater amplitudes than naturally occurring microseisms of similar spectral characteristics. In addition to the type of generating machanism, the character of microseisms is also affected by the ground over which microseismic energy travels.

The purpose of this thesis is to determine the directional characteristics, velocities, and particle motions of short-period microseisms in the limited frequency range of 2 to 5 cps.

Previous Research on Short-Period Microseisms

Ramirez (1948) noted the existence of 2 to 5 cps microseisms near St. Louis, Missouri, and summarized the previous work on short-period microseisms. Walsh (1955) presented the results of an investigation into the origin of 2 to 5 cps microseisms near St. Louis. Of particular interest in his study was a plot of microseismic intensity versus local time of day. This plot showed that the highest intensity occurred between the hours of 7:00 AM and 5:00 PM local time. He related the high microseismic intensity to increased atmospheric pressure micro-oscillations. Heinrich et. al. (1957) extended this study on short-period microseisms near St. Louis by using a tripartite network. Their results indicated the existence of two dominant periods. These were 0.6 and 0.3 seconds. The 0.3 second period group had phase velocities ranging from 490 to 610 ft/sec.

Wilson (1953) presented the results of an extensive study in England on ground vibrations in the frequency range of 1 to 200 cps. He concluded that in order to measure natural background noise it was necessary to choose a location over two miles from a city or large machinery. He measured phase velocities ranging from 682 to 1290 ft/sec for 4 cps microseisms and

ranging from 570 to 2800 ft/sec for 6 to 7 cps microseisms. The particle motions he observed were of the Rayleigh type and his other observations confirmed that microseisms in the frequency range of 4 to 7 cps were surface waves.

Japanese researchers (Kanai et. al. 1951, 1957a-f, 1961) made an extensive study of short-period microseisms in which they related the observed character of the waves to the subsoil. Their period predominance curves exhibited either a single large peak, several peaks, or a flat curve. These corresponded to a thin layer of alluvium, several meters of alluvium, and alluvium over 25 meters thick, respectively. Also, on firm (rigid) ground the observed curves had peaks between the periods of 0.1 and 0.3 seconds whereas on soft (less rigid) ground the curves had peaks between the periods of 0.4 and 0.6 seconds. In tripartite measurements, Akamatu (1961) found a dominant frequency and velocity distribution particular to every observation point. In velocity and direction of approach measurements, the regular waves gave the most consistent results. Irregular and inconsistent results were attributed to the interference of waves from different directions. Particle motion hodographs were very irregular. Elliptical orbits in the vertical plane were attributed to Rayleigh type waves and elliptical

orbits in the horizontal plane were attributed to the arrival of out-of-phase surface waves from different directions. Many of his examples contained both Rayleigh and Love type waves. Judging from the orbits, wavelengths, velocities, and directions of wave propagation, the short-period microseisms showed the characteristics of surface waves controlled by the elastic properties of the ground.

Frantti et. al. (1962) measured the amplitude spectrum of seismic noise between 0.5 and 31 cps at a number of locations throughout the United States and Canada, and consistently found an anomalous peak near 2 to 3 cps. In a more extensive study of seismic noise in the frequency range of 0.2 to 100 cps by Frantti (1963), diagrams of particle velocity versus frequency again showed the anomalous peak near 2 or 3 cps. Figure 1 shows the anomalous peak in his measurements obtained at Magdalena and Truth or Consequences, New Mexico. Particle motion studies indicated Rayleigh type waves but often the orbits were complex.

The only previous study of short-period microseisms at Socorro, New Mexico, was completed in 1963 by Lewis Ballenger (1963). He used the tripartite method to determine wave directions, velocities, and frequencies, but found no significant relationship between these

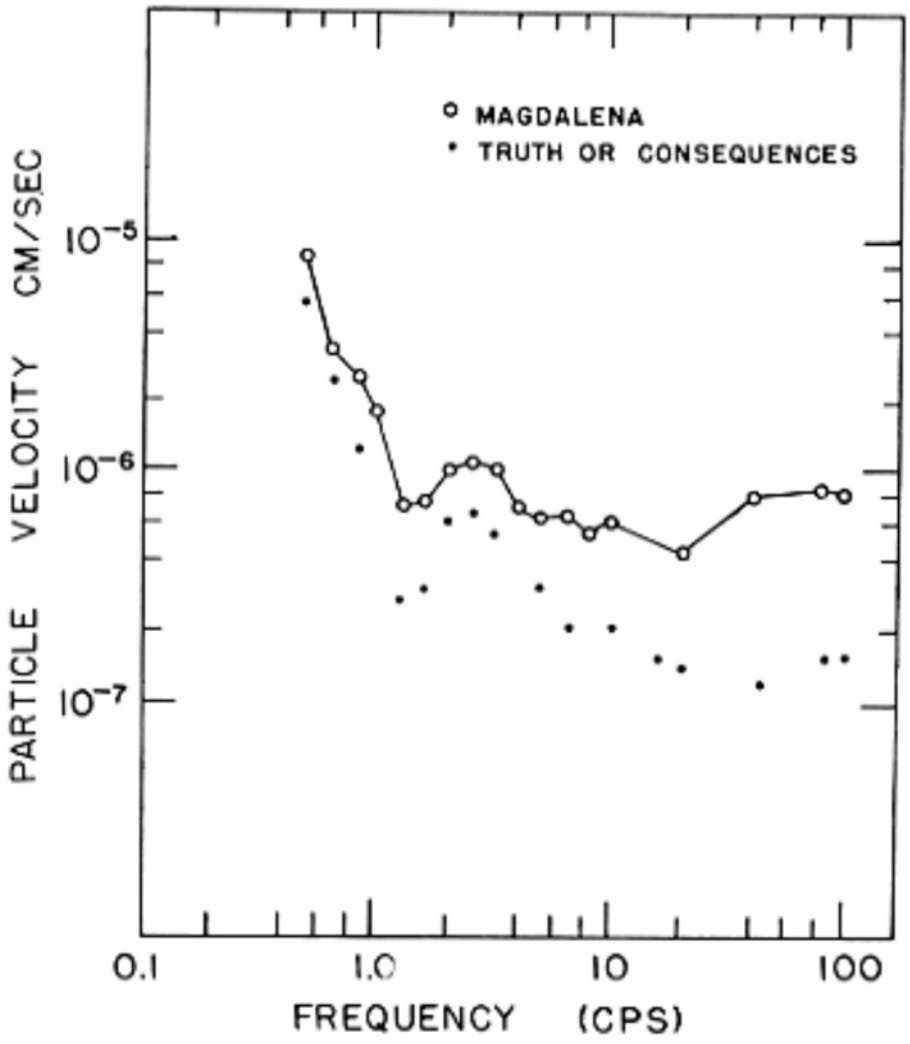

Figure 1. High-frequency earth noise spectra at Magdalena and Truth or Consequences, New Mexico, (from Frantti, 1963).

parameters. His velocity values ranged in the most part from 900 to 1350 ft/sec and his frequency values showed mean and most probable values ranging from 2.9 to 3.3 cps.

In summary, the previous work indicates or shows that the short-period microseisms possess the following six characteristics. First, their origin is primarily industrial with only a few attributed to natural causes. Second, their intensity increases during the daylight hours. Third, the short-period seismic noise spectra possesses anomalous peaks near 2 or 3 cps which show a relationship to the elastic characteristics of the ground. Fourth, the velocities show a large spread in values. Fifth, the particle motions are complex. Sixth, the large spread in velocities and the complexity of the particle motions indicate that in many instances microseisms represent a combination of waves from many different directions.

Instrumentation

The instruments used to obtain tripartite and three-component records of microseisms in the frequency range of 2 to 5 cps consisted of (1) three matched transducers of the electromagnetic type (Willmore seismometers), (2) three pre-amplification units, (3) one eight-channel amplifier and recorder unit, and (4) an oscilloscope. These were arranged as shown in figure 2.

The Willmore seismometers had free oscillation periods of about 0.7 seconds and were operated with damping near 0.7 critical. The open circuit response of the Willmore seismometer was one volt/unit ground velocity of one cm/sec. The amplifier and recorder sensitivity of 2.2×10^{-6} volts/cm of pen displacement was determined directly by comparing a known input signal to pen displacement. The frequency response was as shown in figure 3.

Tripartite records were taken from October 12, 1963, to November 22, 1963, and on March 30, 1964. Three-component records were taken from March 2, 1964, to March 19, 1964. These records were recorded during periods of industrial noise (from 8:00 AM to 5:00 PM) and during quiet periods (from 10:30 PM to 3:00 AM and from 4:00 AM to 6:00 AM).

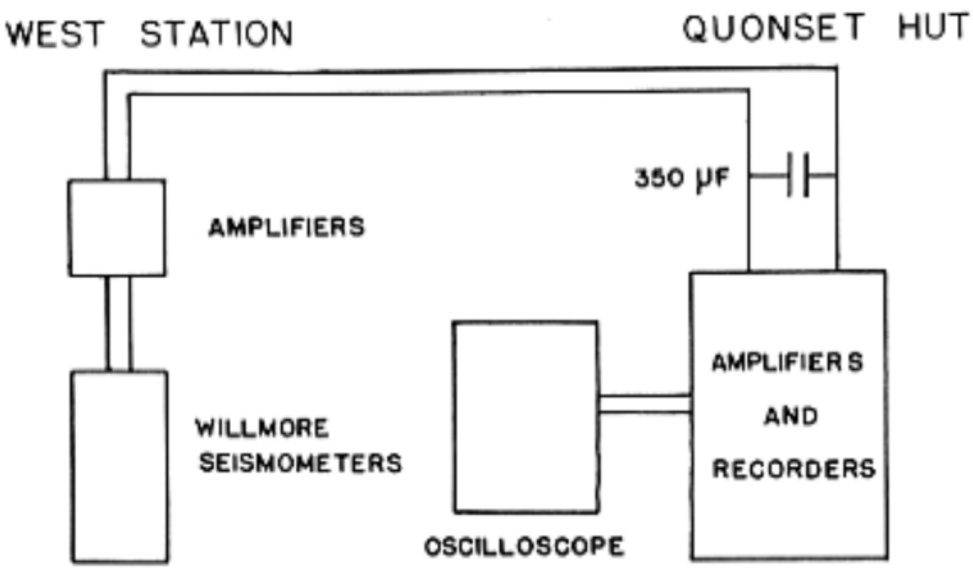

Figure 2. Arrangement of instruments used to record microseisms.

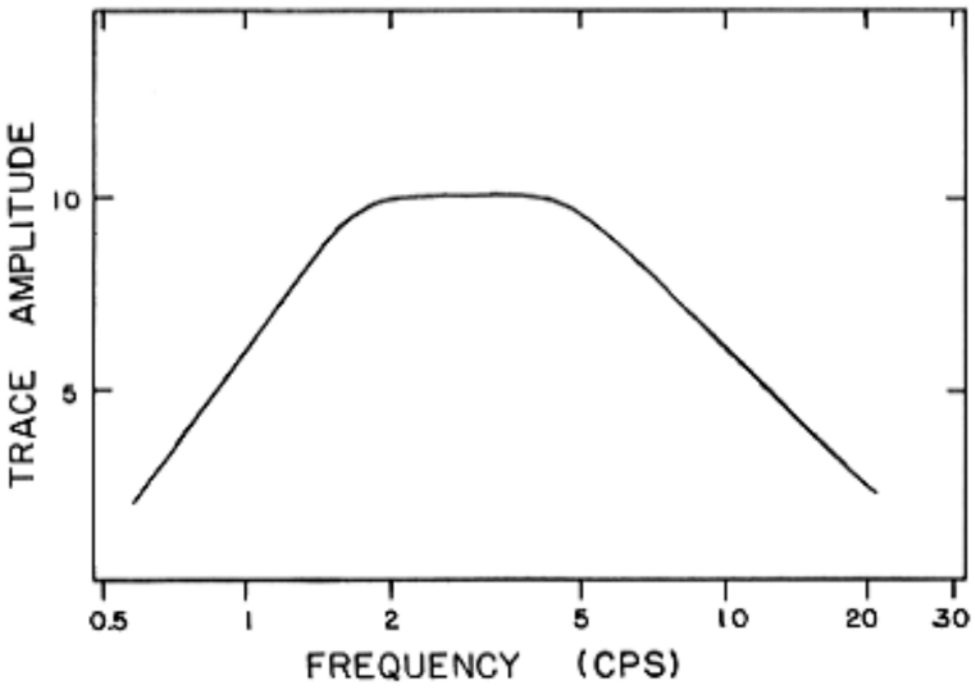

Figure 3. Frequency response of amplifier and recorder system.

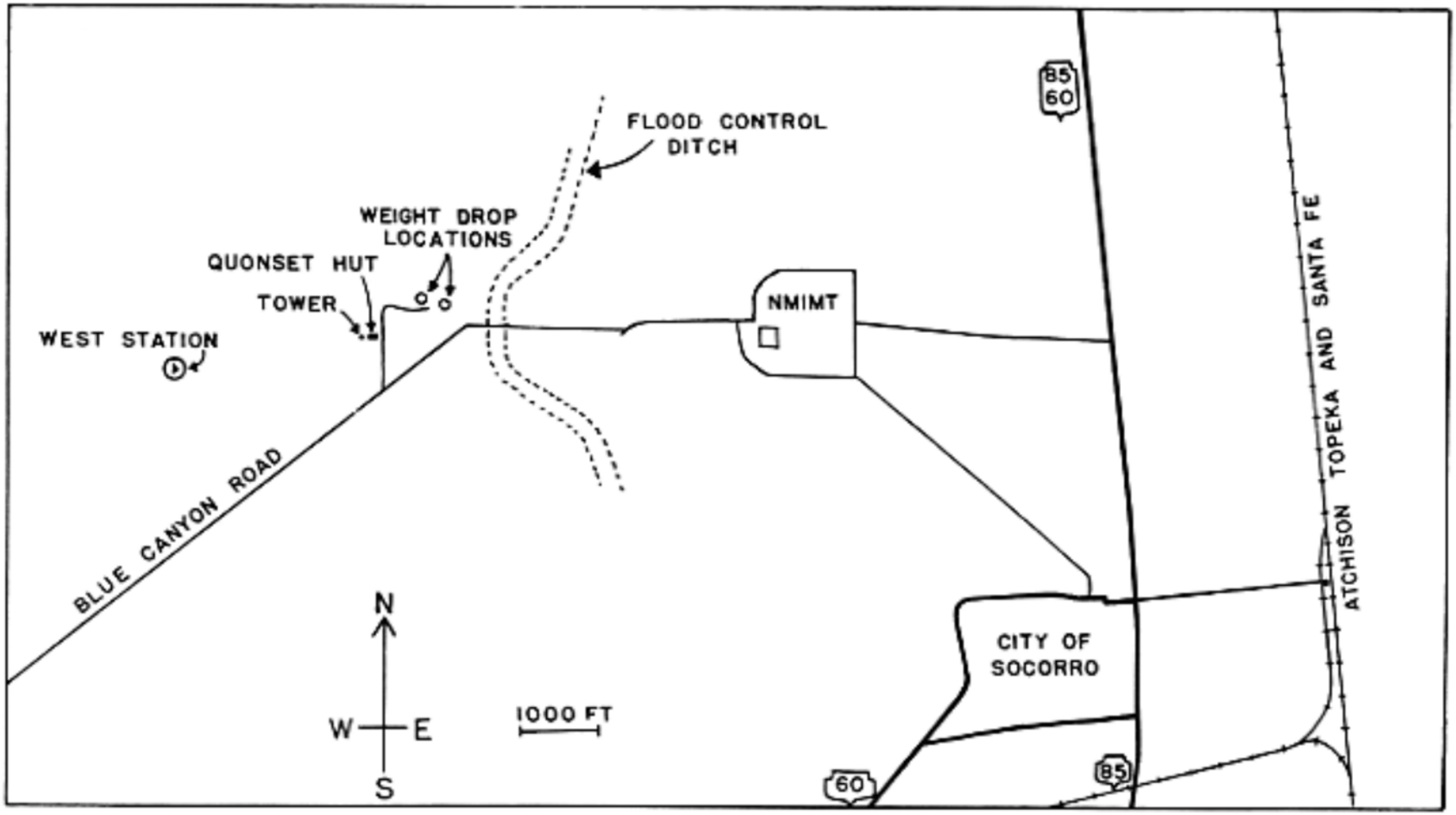

Figure 4. Location of West Station relative to local sources of microseisms.

Both the tripartite network and the three-component array were set up at the West Station, approximately 1.5 mile west of the Research Building on the NMIMT campus (figure 4). The surface material at the West Station is loosely consolidated Quaternary alluvium. The total thickness of Tertiary and Quaternary alluvial deposits beneath the West Station is greater than 2000 feet (A. R. Sanford, personal communication).

The tripartite network consisted of three vertically oriented Willmore seismometers placed at the corners of an equilateral triangle. The north corner of the tripartite network was located at the West Station, the south corner was located 100 feet directly south of the West Station, and the east corner was located 100 feet S-60-E from the West Station. The seismometers were placed in a covered section of 14-inch diameter iron pipe approximately one foot below the surface of the ground. For three-component records, the vertical component was obtained from the north seismometer of the tripartite array and the horizontal components were obtained from two horizontally oriented (east-west and north-south) Willmore seismometers placed near the north seismometer in an enclosed cylindrical cement case approximately 1.5 feet below the surface of the ground.

All records were taken on an eight-channel 12-inch wide strip-chart recorder located in a quonset hut (figure 4) east of the West Station. In tripartite records, channels two, four, and eight from the top of the record were used for one-fifth second time marks. Channels one three, and five recorded vertical ground motion at the north, east, and south stations, respectively. In the particle motion records, channels one, three, and eight were used for one-fifth second time marks and channels two, four, and five recorded the vertical, east-west, and north-south components of ground motion, respectively. Channel six was used for coding the record.

In the three-component recording, a dual-beam oscilloscope was used as a vector seismograph. The upper beam of the oscilloscope was connected to the amplified signals of the vertical and east-west seismometers. The lower beam was connected to the amplified signals of the north-south and east-west seismometers. This made it possible to observe the particle motion directly in vertical and horizontal planes. To record the particle motions, time exposures were taken of the oscilloscope face.

No equalization of trace amplification was performed for the tripartite recording because only the time differences in the phase arrivals and the frequencies

of the microseisms were measured.

Particle motion records, however, did require equalization and the following method was used. The two horizontal seismometers were placed parallel to each other to produce identical signals. Two of the amplifier and recorder systems were successively connected to one of the parallel seismometers. While connected, the mean pen displacements of the two systems were adjusted equal to the mean pen displacement of the third system which was connected to the other horizontal seismometer.

The displacements of the beams on the oscilloscope face were equalized by adjusting the scope sensitivity until straight lines at 45 degrees were obtained. An elliptical figure would indicate unequal phase changes in the amplification systems. No phase difference could be detected.

Methods of Analysis

Selecting Samples

One of the main obstacles in the study of microseisms has been the lack of signal coherence from station to station (Donn and Blaik, 1953). In this study only those records containing 2 to 5 cps microseisms of sufficient amplitude and coherence for analysis were retained. Incoherence was assumed to be caused by the interference of surface waves of different frequencies and directions (Akamatu, 1961). To avoid the complexities of multiple waves only sections of the record where the microseisms appeared coherent for a number of cycles were considered. Occasionally, some coherent microseisms were rejected because of a beat phenomena in which the combination of two or more frequencies resulted in alternating phases of reinforcement and cancellation of the amplitudes.

Picking Frequencies and Corresponding Phases

To determine frequencies, intersections of the trace with a median line, or the position of the peaks projected to a median line, were picked for a coherent series of microseisms. These were then compared to a previously measured interval-frequency scale as

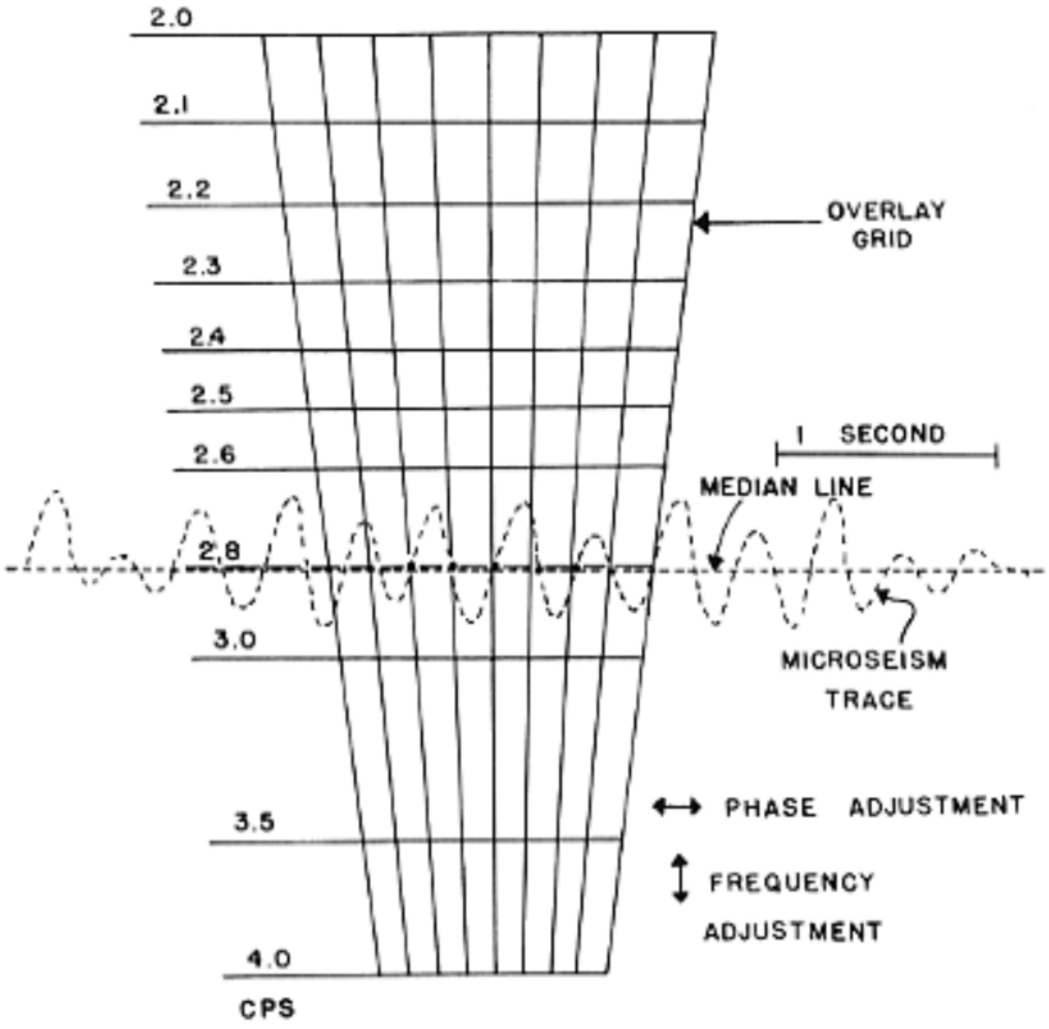

Figure 5. Application of the phase and frequency grid to the determination of the frequency and phase position of a series of microseisms.

illustrated in figure 5. The best fit for a sequence of oscillations was chosen. The vertical scale gives the dominant frequency of the sequence. Because weak signals of different frequencies were invariably present to an unknown extent, the dominant frequencies were extimated to the nearest 0.1 cps. Where a sequence of oscillations could be identified at all three of the tripartite stations, the best phase position for measurement of time differences was determined by the position of the trace on the horizontal scale.

Tripartite Analysis

Determination of direction of approach of the microseisms was based on the ratio (Schuyler, 1955)

$$R = \frac{T_1 - T_2}{T_1 - T_3},$$

where T_1, T_2, and T_3 are the arrival times of a particular phase at the three stations. Figure 6 shows the relationship between R and the angle of approach θ. The equation relating R to θ was plotted (figure 7) to facilitate the determination of θ directly from R.

The phase velocity was determined from the diagram in figure 7 which relates the phase velocity to the angle of approach and the maximum time difference between stations.

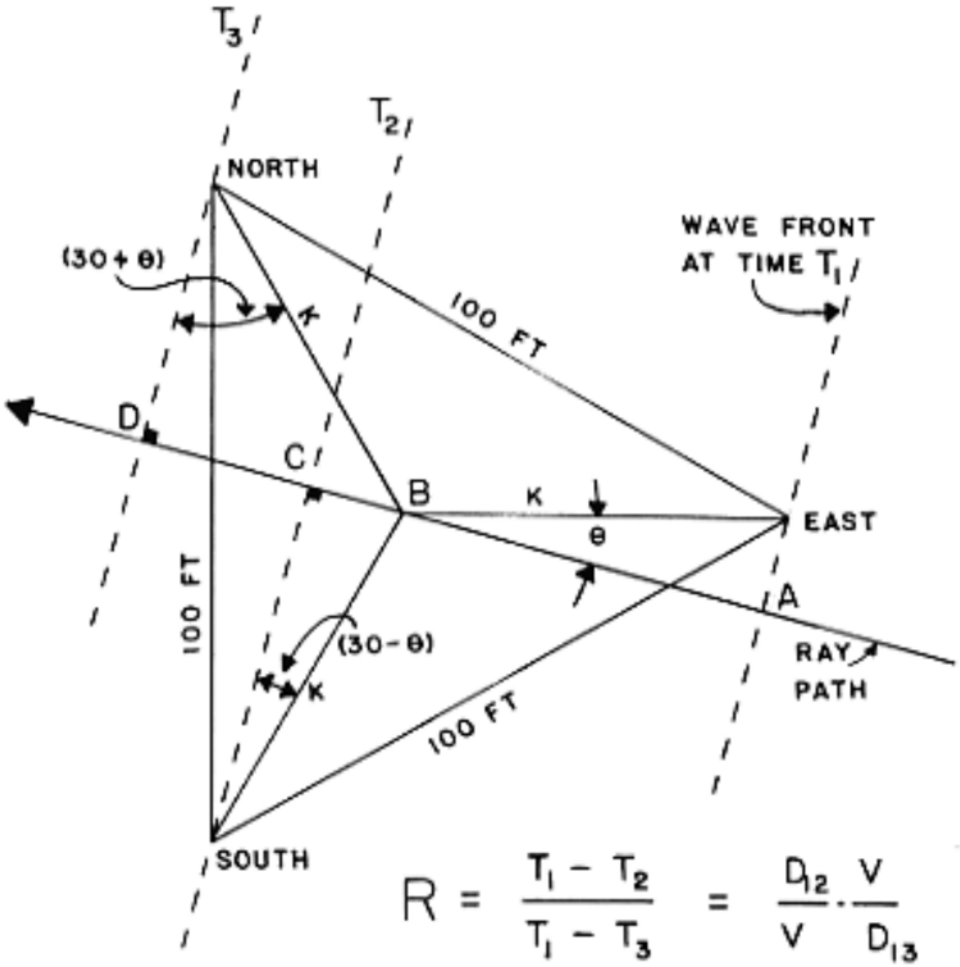

$$R = \frac{T_1 - T_2}{T_1 - T_3} = \frac{D_{12}}{V} \cdot \frac{V}{D_{13}}$$

WHERE

$$D_{12} = \overline{AB} + \overline{BC} \quad \text{AND} \quad D_{13} = \overline{AB} + \overline{BD}$$

$$D_{12} = K\text{Cos}(\theta) + K\text{Sin}(30-\theta)$$

$$D_{13} = K\text{Cos}(\theta) + K\text{Sin}(30+\theta)$$

$$R = \frac{\text{Cos}(\theta) + \text{Sin}(30-\theta)}{\text{Cos}(\theta) + \text{Sin}(30+\theta)} \qquad V = \frac{D_{13}}{T_1 - T_3}$$

Figure 6. Derivation of the equations for angle of approach and velocity of surface waves.

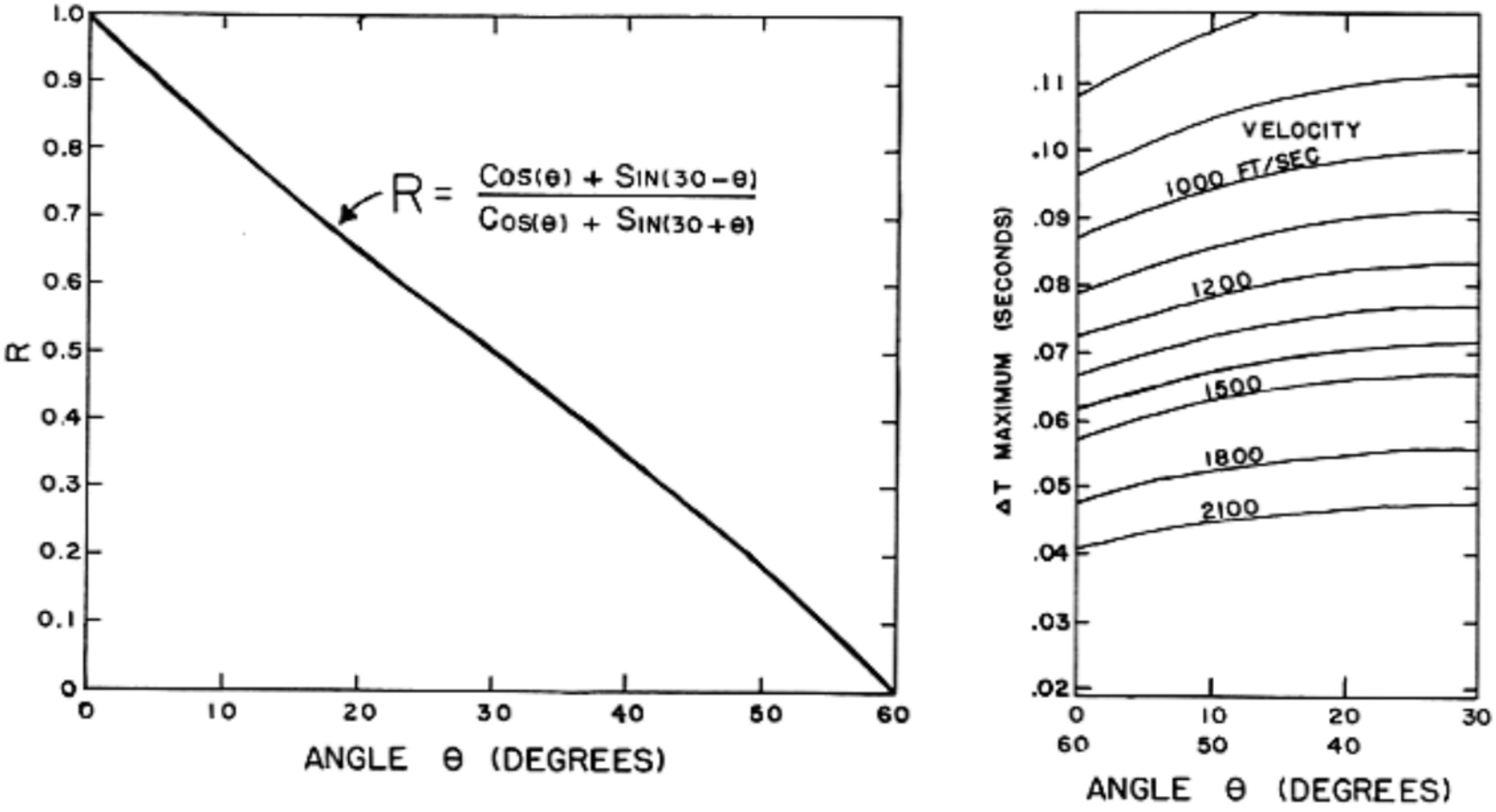

Figure 7. Graphs used to calculate the angle θ and the velocity of surface waves.

Errors in Analysis

In order to estimate the errors in direction of approach, frequency, and velocity, (independent of choice of phase), two independent calculations of 20 pre-picked phases were performed. The difference between these two calculations yielded a standard deviation of 4.4 degrees in angle of approach, 0.076 cps in frequency, and 107 ft/sec in velocity.

Particle Motion Analysis

The output of the Willmore seismometers is a measure of particle velocity and thus the amplitude of the recorder trace was proportional to the frequency of the particle motion. Because there was only a small variation in the frequency of the microseisms, the particle velocity hodographs were considered nearly equivalent to the particle motion hodographs.

Particle motion hodographs were made directly from the three-component records by reading amplitudes at small time intervals along each of the three traces. The amplitudes at corresponding points in time were then plotted to determine particle motion in the vertical and horizontal planes.

In addition to the three-component strip-chart records, photographs were made of the particle motion registered by the oscilloscope. As these photographs

were quite small, enlargements were made with an opaque enlarging projector.

Presentation and Discussion of the Data

Sources of Short-Period Microseisms

Short-period microseisms are never constant in magnitude but vary relative to the distance from and character of the sources. In over 100 hours of recording time, the short-period microseisms never completely disappeared. The trace always exhibited a small component of natural or industrial microseisms. The only microseisms which could be associated with a natural source occurred during an unusually strong wind from the north-west and consisted primarily of high-frequency noise. Industrially produced microseisms generally dominated all the records taken.

The velocity, direction, and wave-form characteristics of short-period microseisms were determined for the most part from records of trains for the following reasons. First, the trains generated microseisms of the greatest magnitude. Their amplitude was thirty times greater than the average microseism level at night. During the day, train microseisms stood above other microseisms, even during the periods of heavy and close vehicular traffic. Second, the train could be sighted from the tower near the quonset hut when its position was between 1.0 mile south of the station to 2.6 mile north of the station at Socorro.

Third, the train microseisms were consistent in character and available throughout the total period of recording. Fourth, the microseisms were in the frequency range of 2 to 5 cps at the West Station.

Another prevalent source of short-period microseisms was vehicular traffic. At night large trucks passing through the city of Socorro on highways US 60 and US 85 generated increased microseismic noise for periods having average durations of eight minutes. Their magnitude was seldom more than five times the magnitude of quiet periods during the night. A general increase in the vehicular traffic was responsible for the increased level of microseisms during the daytime. Records of traffic on Blue Canyon road (at a distance of 1500 feet to more than 5000 feet from the West Station-see figure 4) confirmed that vehicular traffic contributed to the level of microseisms during the day. While a vehicle was close to the West Station, the microseism amplitude was high and contained a large portion of high-frequency (above 10 cps) noise. As the vehicle moved away from the West Station, the high-frequency components diminished considerably and the character of the record approached that of normal daytime noise.

Large construction equipment produced microseisms even more effectively than normal vehicular traffic. During part of the recording period large earthmovers

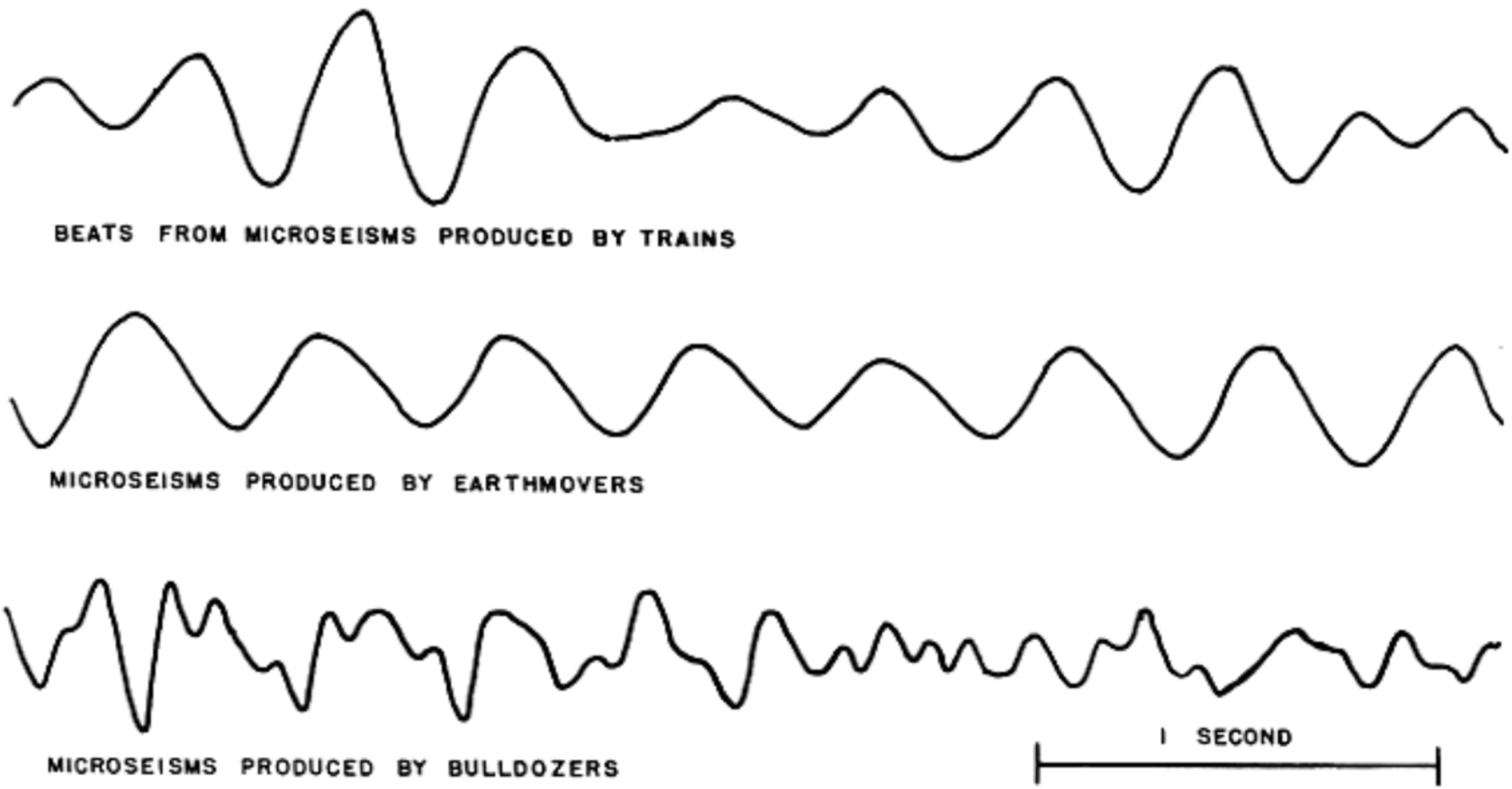

Figure 8. Sample records of microseisms generated by earthmovers, bulldozers, and trains.

("Euclids") and bulldozers were being used in the construction of a flood control ditch around the city of Socorro (figure 4). The bulldozers engaged in digging and moving of the ground produced a very irregular sequence of waves (figure 8). The transportation of the material in "Euclids" produced a sequence of waves (figure 8) having a frequency roughly equal to the bounce frequency of the "Euclids".

Direction Studies

In the analysis of direction of approach, four records of microseisms generated by different trains were examined. Direction determinations were made in time intervals of approximately one minute or less and the resulting plots are shown in figures 9, 10, 11, and 12. In figures 10 and 11 the position of the train was determined at one point in its travel down the valley. From N-40-E to S-50-E the spread in the direction determinations was the same order of magnitude as the angle subtended by the train. This consistency in the direction determinations broke down near S-50-E (figure 9). When the train was south of an angle of S-50-E, the microseisms arrived randomly from directions ranging from near S-50-E to south. Figures 11 and 12 show a similar but more gradual breakdown in the consistency of direction of arrival from N-40-E to N-70-E.

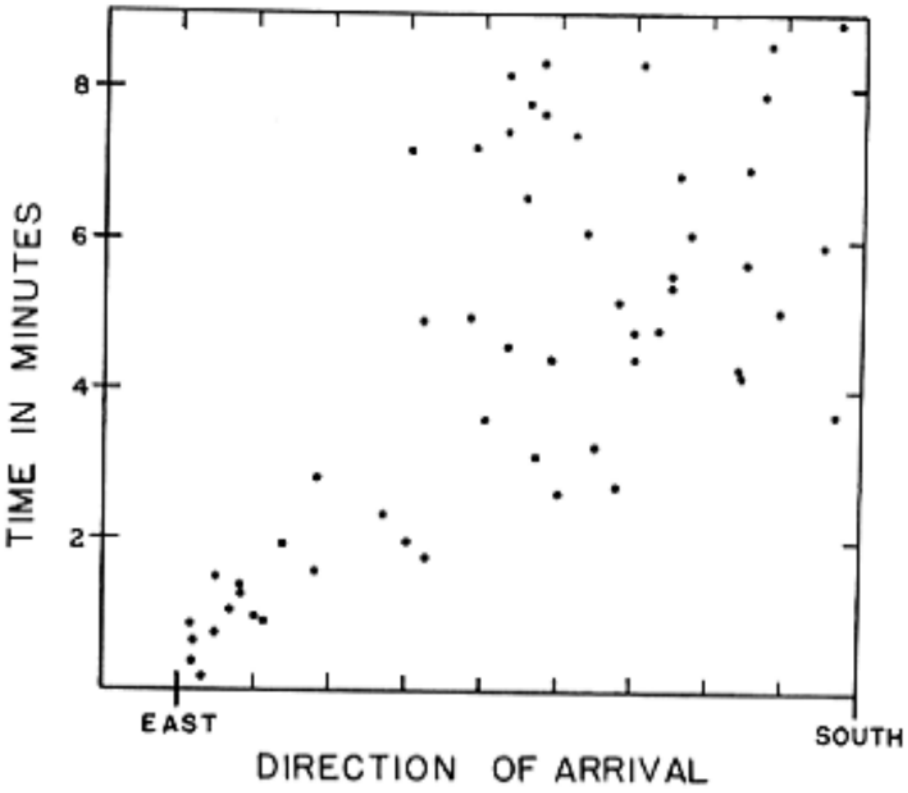

Figure 9. Direction determinations of a train going south on October 14, 1963.

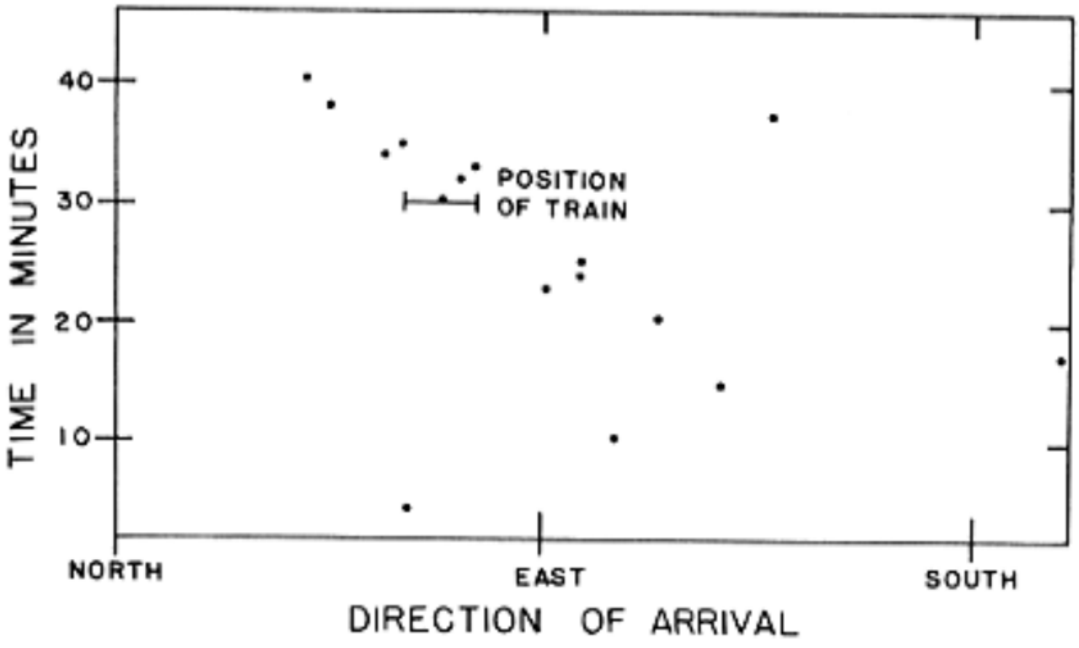

Figure 10. Direction determinations of a train going north on November 3, 1963.

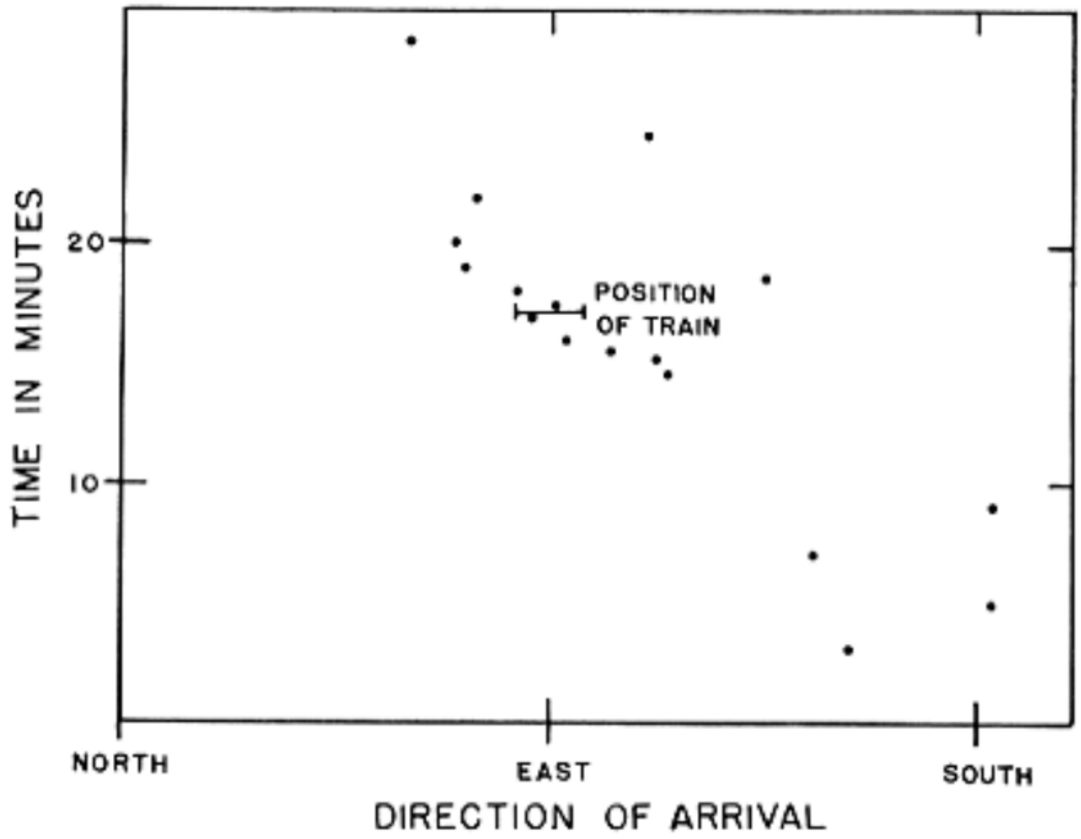

Figure 11. Direction determinations of a train going north at 2:00 PM on November 2, 1963.

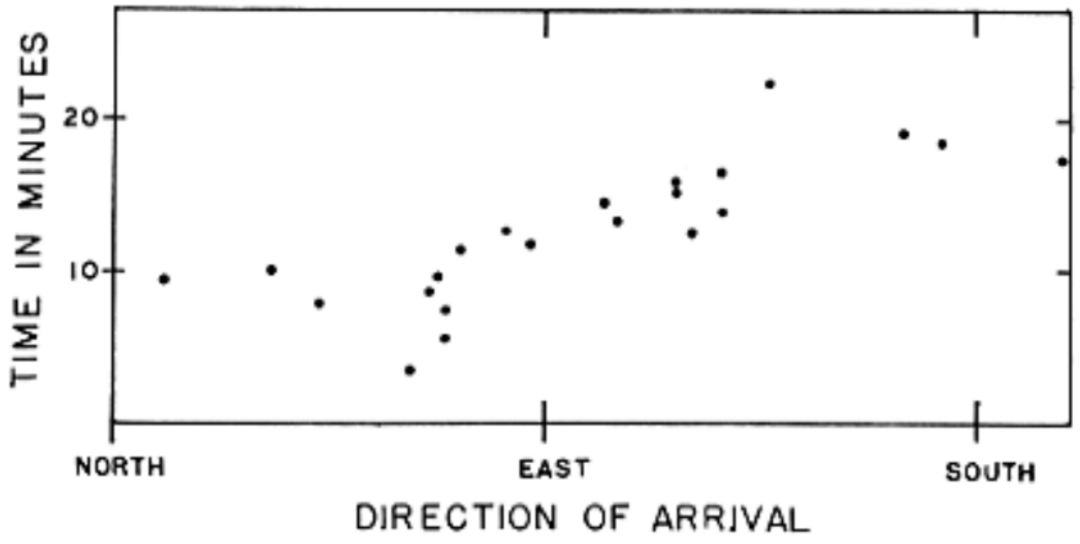

Figure 12. Direction determinations of a train going south at 5:00 AM on November 2, 1963.

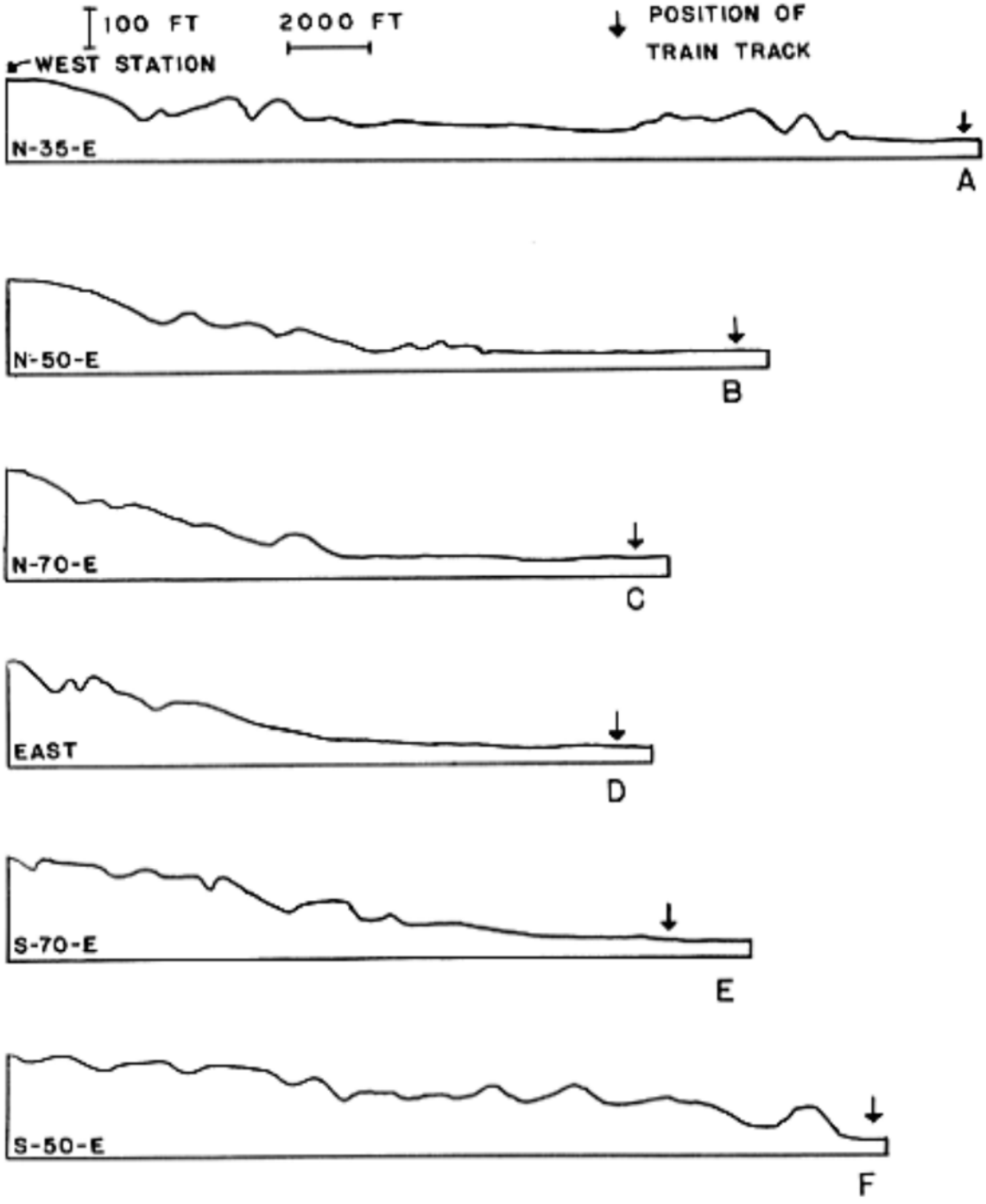

Figure 13. Radial topographic cross sections from the West Station.

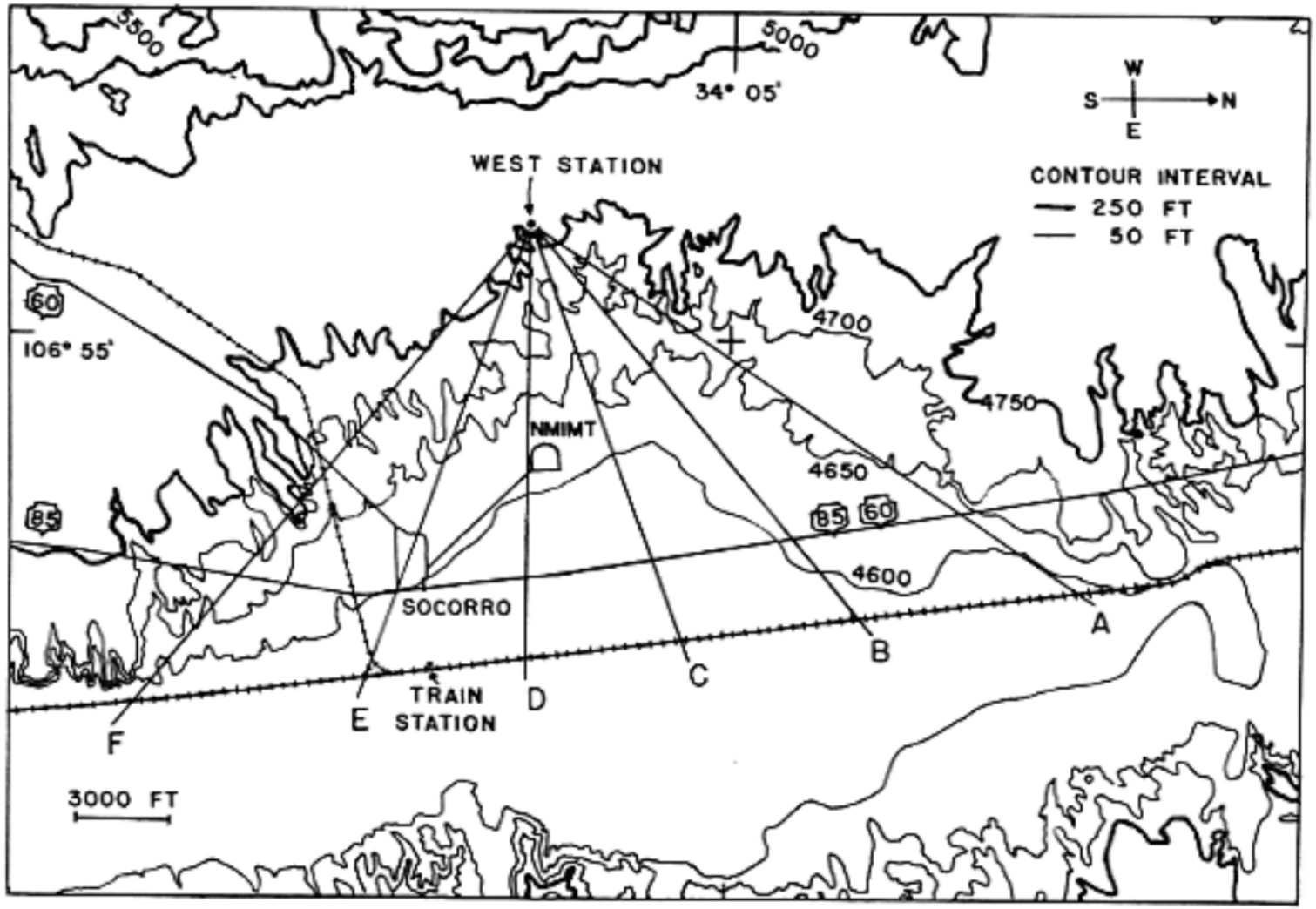

Figure 14. Map showing the relationship of the West Station to the topography and train track.

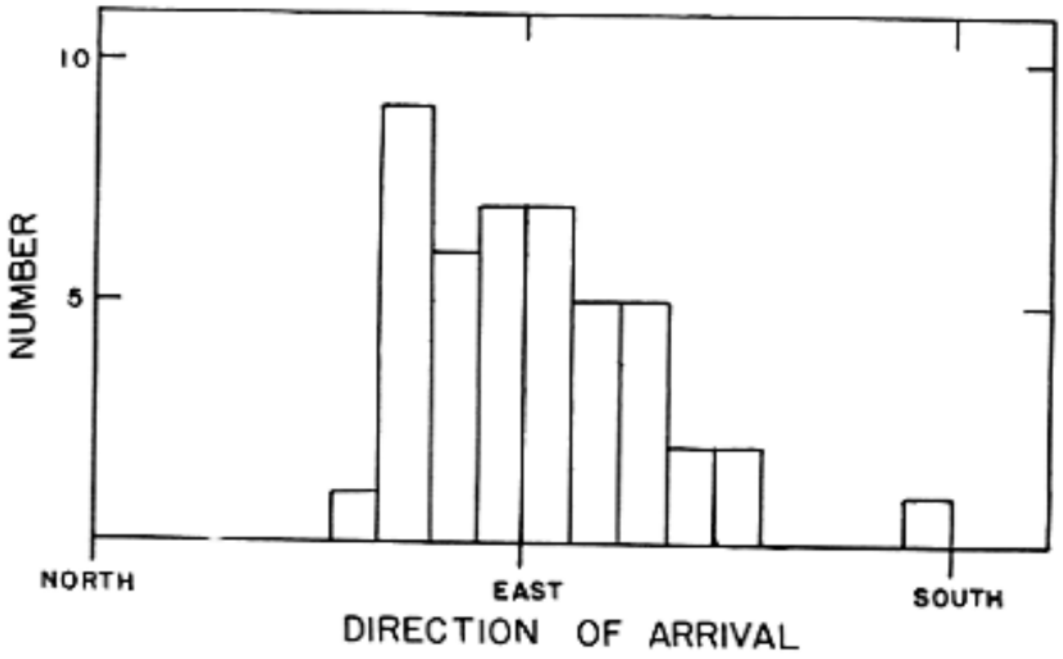

Figure 15. Directions of arrival determinations on non-train microseisms.

The zones outside of N-50-E to S-70-E represent areas where the topographic relief increases. This is evident on inspection of the topographic cross sections (figure 13) and the topographic map (figure 14). The cross sections at N-35-E and S-50-E do not show the approximately 7000 foot wide flat area from the train track towards the West Station as do the other cross sections. Knopoff (in Gutenberg, 1958) reported that topography in excess of one-fourth wave length seriously attenuates surface waves. For microseisms in the frequency range of 2 to 5 cps travelling at a velocity of 1200 ft/sec, the one-fourth wave lengths are 50 to 150 feet. The topographic relief between N-50-E and S-70-E seldom exceeds 50 feet whereas the cross sections at N-35-E and S-50-E show considerable relief in excess of 50 feet. Thus outside the zone from N-50-E to S-70-E the increased topographic relief is sufficient to attenuate and scatter the train microseisms.

All of the non-train microseisms in the frequency range of 2 to 5 cps came from the directions N-60-E to S-40-E (figure 15). These microseisms were generated either by flood control construction or traffic in and through Socorro.

Frequency Determinations

The relative prevalence of the frequencies in the microseisms studied was determined by plotting the number of measurements against frequency (figures 16a through 16d). In 87 determinations of frequency on each of the three components of a single train microseism record, peaks were found at 2.9 and 3.4 cps on the north-south component (figure 16a) and at 3.0 and 3.5 cps on the east-west (figure 16b) and vertical (figure 16c) components. In 132 frequency measurements of train microseisms (same samples as used in the direction determinations), peaks occurred at 2.9 and 3.4 cps (figure 16d). In all cases the peak near 2.9 cps was greater than the peak near 3.4 cps. The vertical displacement at a single point, resulting from the intersection of surface waves of different frequencies, is given by the equation

$$w = 2A \cos((f_1-f_2)\pi t) \cos((f_1+f_2)\pi t).$$

For the frequencies of 2.9 and 3.4 cps, this equation yields a beat period of 2.0seconds which corresponds to 6.3 cycles/beat. Beats having an approximate duration of 6.3 cycles (figure 8) were common in train microseisms.

Velocity Determinations

From tripartite records, one can only measure phase velocity, the velocity with which a peak or

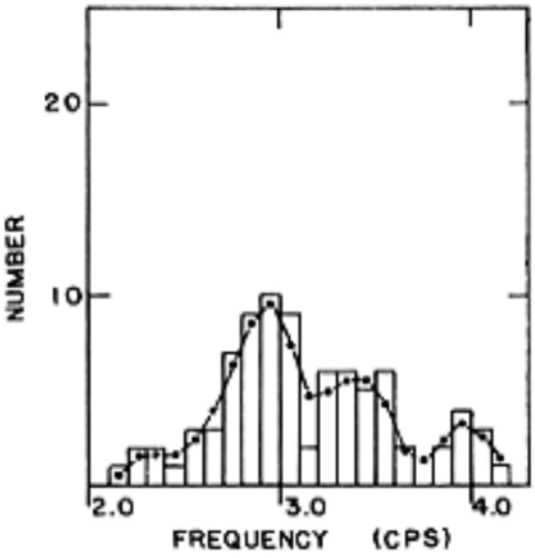

Figure 16a. Frequency determinations on the N-S component of a train record, March 6, 1964.

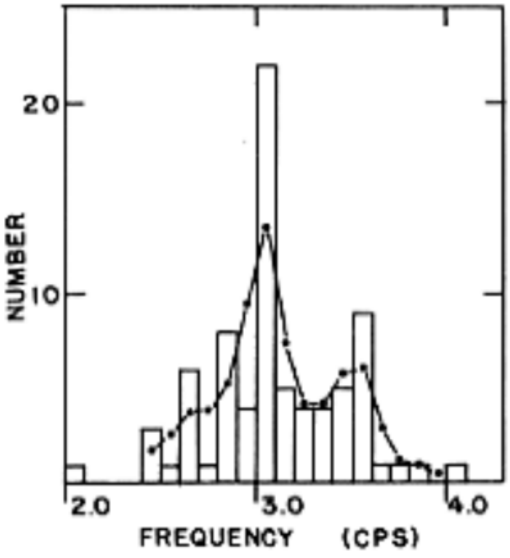

Figure 16b. Frequency determinations on the E-W component of a train record, March 6, 1964.

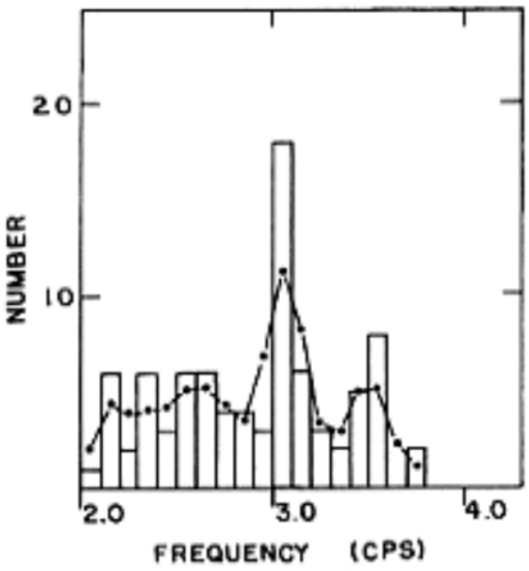

Figure 16c. Frequency determinations on the vertical component of a train record, March 6, 1964.

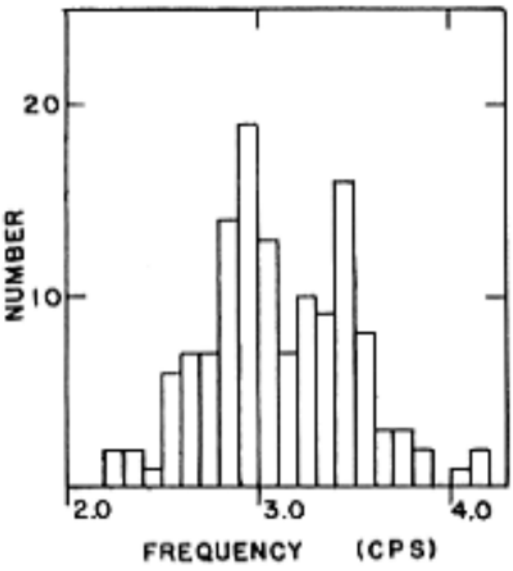

Figure 16d. Frequency determinations of train microseisms for which direction was determined.

particle displacement traverses the tripartite network. Figure 17 shows the distribution of 127 phase velocity determinations made from train microseisms. The distribution extends from 1000 ft/sec to 2200 ft/sec and has a peak at 1350 ft/sec. Several factors contributed to this spread in velocity values.

First, the 107 ft/sec standard deviation of the errors in analysis could account for most of the spread about the peak near 1350 ft/sec. However, the large number of determinations below 1200 ft/sec and above 1500 ft/sec can not be explained in terms of a normal distribution about this peak.

Second, the intersection of two or more surface waves of identical character produces an interference pattern which propagates along the ray bisecting the directions of arrival of the individual waves. The resulting peaks correspond to the intersection of the peaks of the individual waves. The peaks travel a distance $\overline{AB}$ (figure 18) in time Δt while the individual waves travel a distance $\overline{BC} = \overline{BD}$ in the same time. As a result of this interference the velocity of the combined wave is greater than the velocity of the individual waves by a factor of Sec $(\theta/2)$ (Donn and Blaik, 1953). Because interference of this type does not alter the character of the record at a given station (Leet, 1949), this type of combination of

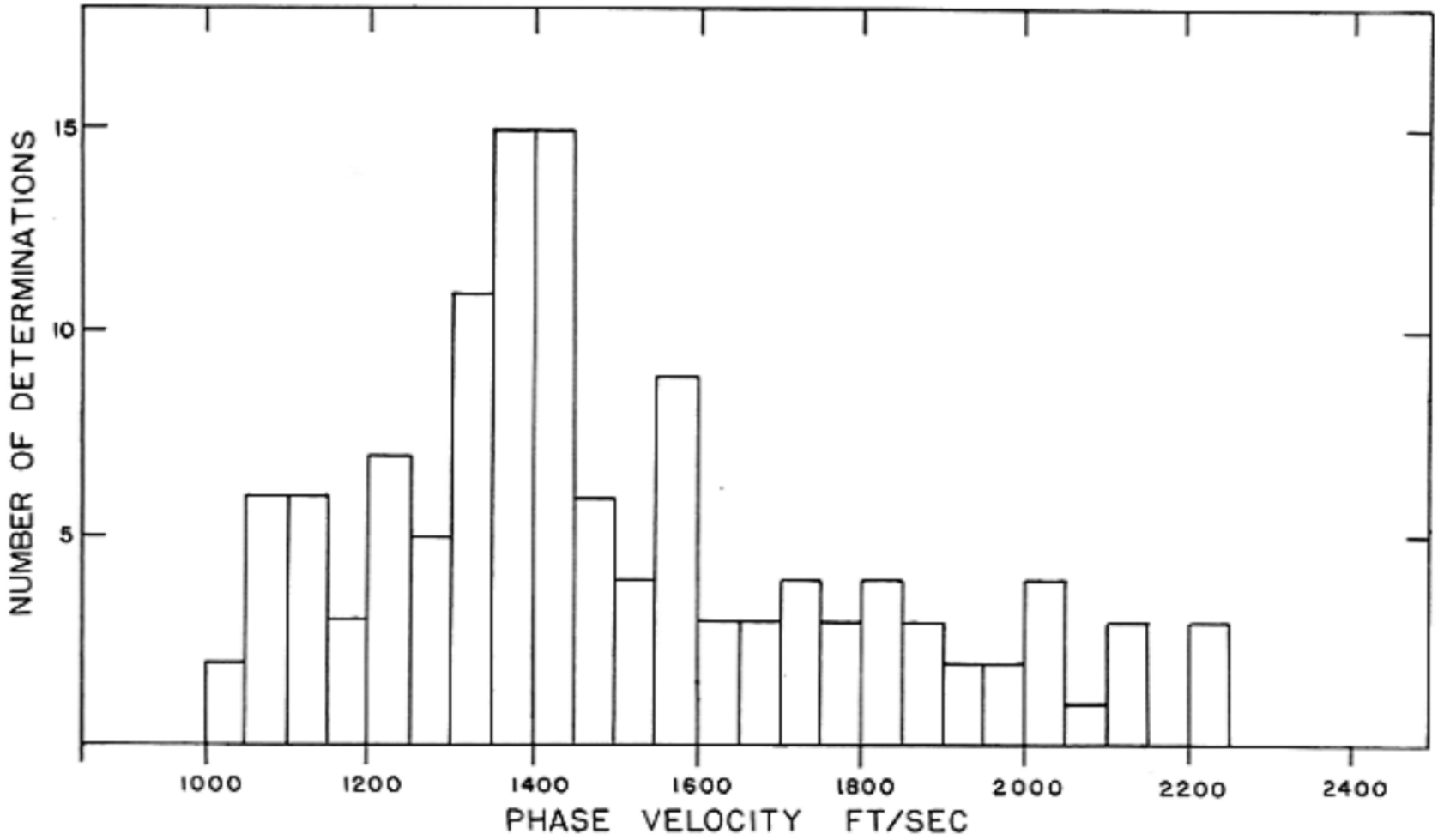

Figure 17. Distribution of phase velocities of train microseisms.

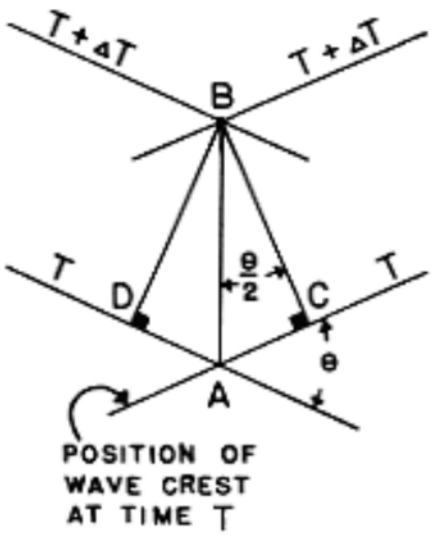

$$V = \frac{\overline{BC}}{\Delta T} = \frac{\overline{BD}}{\Delta T}$$

$$V_{AP} = \frac{\overline{AB}}{\Delta T}$$

$$\frac{V}{V_{AP}} = \frac{\overline{BC}}{\overline{AB}} = \cos\left(\frac{\theta}{2}\right)$$

$$V_{AP} = V \sec\left(\frac{\theta}{2}\right)$$

Figure 18. The combined phase velocity of two intersecting waves.

microseismic waves can not be distinguished from a single wave.

Third, past experience (Donn and Blaik, 1953) has shown that it is difficult to correlate microseismic waves from station to station when the distance between stations is greater than one wave length. The dimensions of the tripartite network used corresponded to approximately a one-fourth wave length of the 3 cps microseisms. Frequencies higher than 10 cps correspond to wave lengths less than 100 feet and would not correlate well between these stations. For this reason high-frequency noise, superimposed on the dominant 3 cps frequencies, introduced a random error in the velocity and direction determinations. The interfering high-frequencies may have originated from close traffic, wind, or the train itself.

Fourth, body waves would, if present appear in the higher velocity ranges of figure 17. However, since the energy of surface waves attenuates with distance (r) as $1/r$ due to geometrical spreading compared to $1/r^2$ for body waves, it is unlikely that the train microseisms contained a large body wave component at the distances involved.

Comparison of Microseism and Rayleigh Wave Velocities

Rayleigh wave velocities were obtained from records

of ground motion produced when a 5000 pound weight was dropped from a height of 25 feet. The weight dropping took place at a distance of 3400 feet and at a direction of N-75-E from the West Station.

The Rayleigh wave component of the weight drop record showed dispersion (Officer, 1958, pp. 66-72). The group velocities were obtained by dividing the distance to the source by the travel time for a particular frequency. The phase velocities were measured from the tripartite records. The resulting plots of velocity versus the period are shown in figure 19.

The phase velocity of the Rayleigh wave extends from 1200 ft/sec for a wave period of 0.2 seconds to 1400 ft/sec for a wave period of 0.37 seconds. The train microseisms had a peak in the velocity distribution at 1350 ft/sec and a dominant frequency near 2.9 cps. This point corresponds to the phase velocity of the 2.9 cps Rayleigh wave portion of the weight drop record. For this reason microseisms must contain a large component of Rayleigh type motion.

By assuming a Poisson's ratio of 0.25 and a compressional wave velocity of 2050 ft/sec (obtained from the weight drop records), theoretical calculations yield a Rayleigh wave velocity of 1080 ft/sec for the surface material. Curves drawn from the velocity

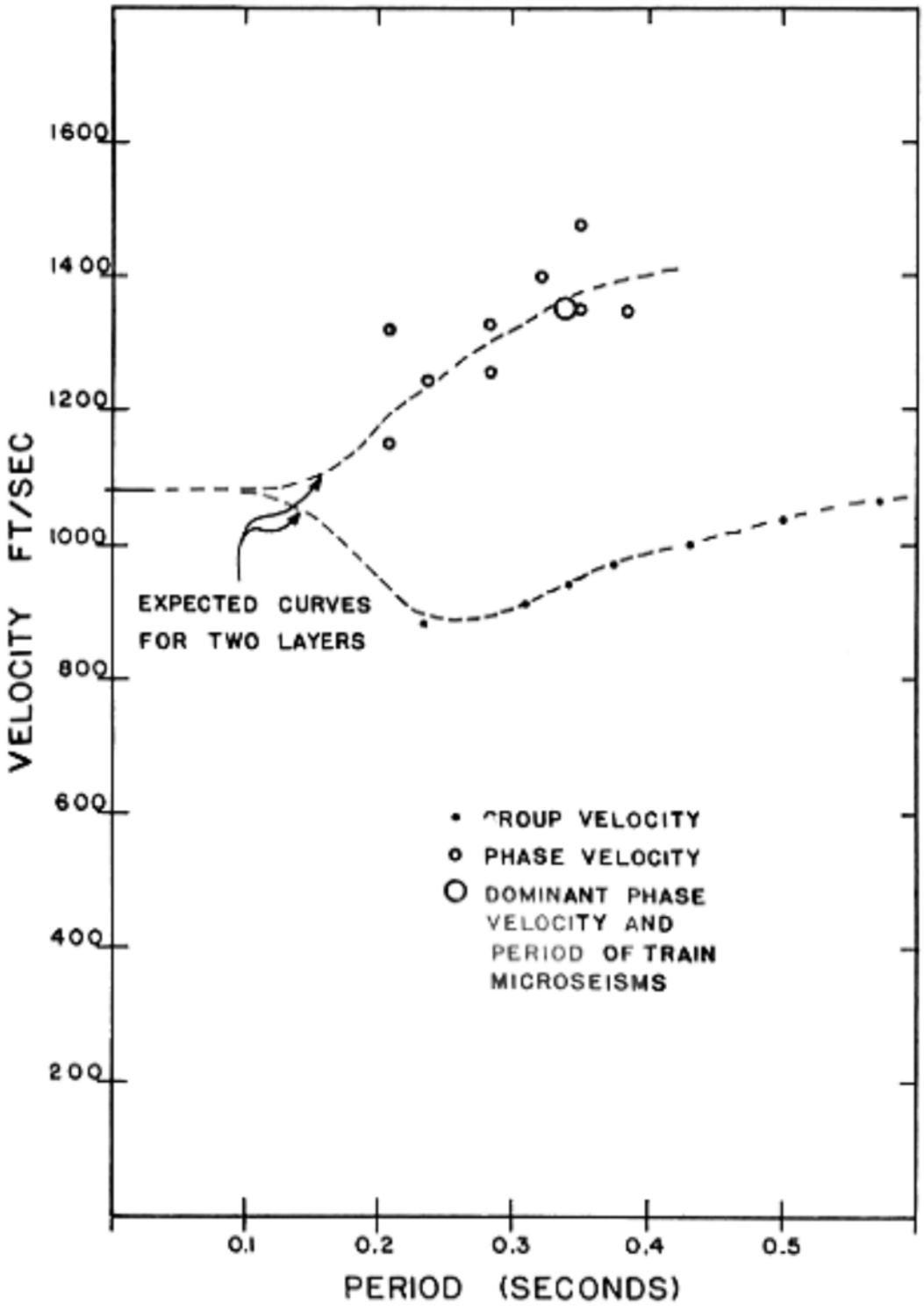

Figure 19. Phase and group velocities of Rayleigh waves from weight drop records.

of 1080 ft/sec at a period of zero seconds through the group and phase velocity points are similar to the expected dispersion curves for a two-layer case (Ewing et. al., 1957, p. 208).

Particle Motions

All previous observations of the particle motion of short period microseisms have yielded complex orbits (Eisler, 1952) in which both Love and Rayleigh type wave components were recognized. The short-period microseisms recorded at the West Station are no exception (figures 20 through 38 and table 1).

Figures 20 through 28c, and 29 through 31 illustrate the particle motion when a strong Rayleigh wave component is present. In all of these except figures 27 and 29 through 31, the major axis is tilted toward the direction of propagation. The first six have a mean tilt of 12 degrees with a spread of 5 degrees. For the same six exomples the ratio of the minor to the major axis of the ellipses averages 0.58 with a spread of 0.16. This compares to the theoretical axial ratio of 0.68. Figures 25 and 27 show an intersection of two Rayleigh waves at angles close to 90 degrees. Portions of the particle motion in the horizontal plane are elliptical. The ellipticity is caused by the combination of the

two horizontal components of the Rayleigh waves (Akamatu, 1961).

Figures 23, 29, and 31 show Love components superimposed on Rayleigh waves and figure 34a shows an isolated Love component. Figures 28d, 30, 32, 33a and 33b are particle motions of a wave type which is almost entirely vertical. Figures 32, 33a, and 33b show this wave alone and figure 30 shows it superimposed on a basic Rayleigh wave form. Wave motion of this type could be the result of two opposing Rayleigh waves or it could represent the second mode of Rayleigh waves (Gutenberg, 1958).

Figures 34b and 35 show motion along an axis which is neither horizontal nor vertical and which in figure 35 appears to change position in time. Rotations and transformations of the wave forms are common in microseisms. Figures 28a through 28d show the transformation of a Rayleigh type wave into wave motion along the vertical axis. Figure 34a and 34b show the transformation of a Love wave to motion along an axis at 45 degrees to the horizontal.

The remaining examples illustrate the very complex particle motions typical of train microseisms. Their complexity was undoubtedly due to a combination of the above described wave types. By choosing the proper frequencies, phase velocities, amplitudes and directions

any continuous particle motion could be constructed from a combination of Love and Rayleigh waves.

Table 1. Source of Particle Motion Figures

The following figures were obtained from the three-component strip-chart records.

Figure 20 is a hodograph of a Rayleigh wave pulse produced by construction equipment.

Figures 34a,b are successive hodographs of a surface wave pulse produced by construction equipment.

Figure 25 is the hodograph for the Rayleigh wave protion of a weight drop record. The north-south trace is too small for analysis.

Figures 21, 22, and 32, are selected hodographs of microseisms produced by trains. The amplitudes of the east-wext traces are too small for analysis.

Figures 28a,b,c,d and 33a,b are successive hodographs of microseisms produced by trains.

The remaining particle motion figures are train microseisms from the enlarged photographs of the oscilloscope face.

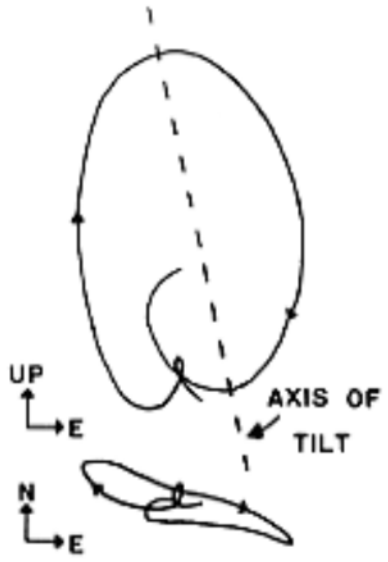

Figure 20.

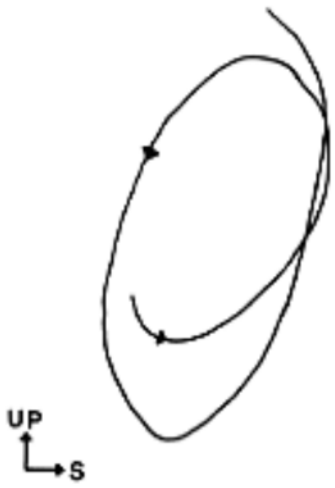

Figure 21.

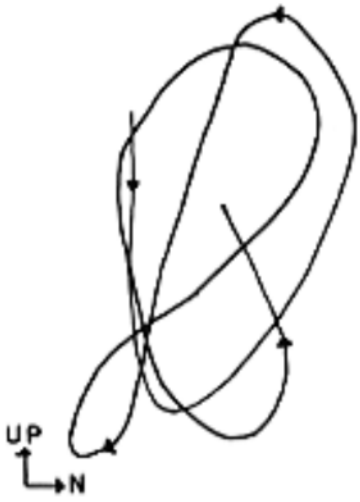

Figure 22.

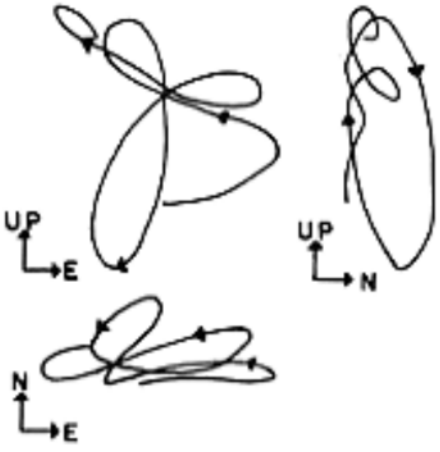

Figure 23.

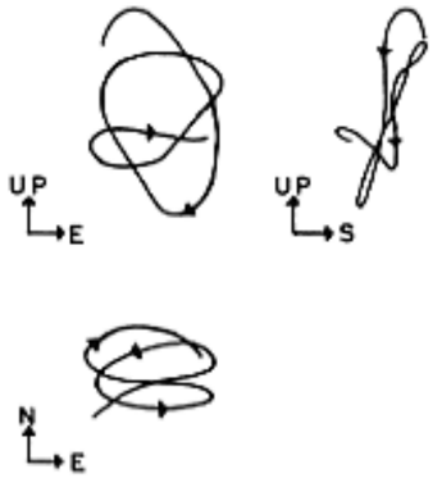

Figure 24.

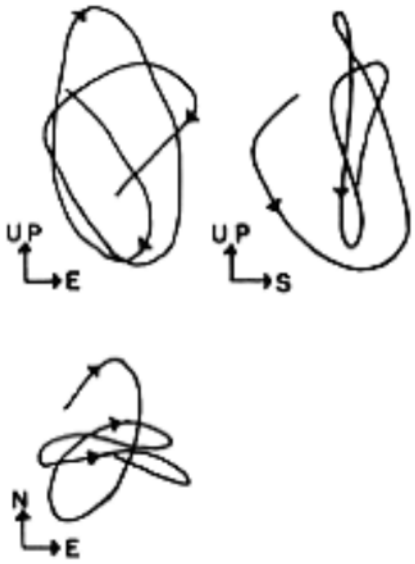

Figure 25.

Figure 26.

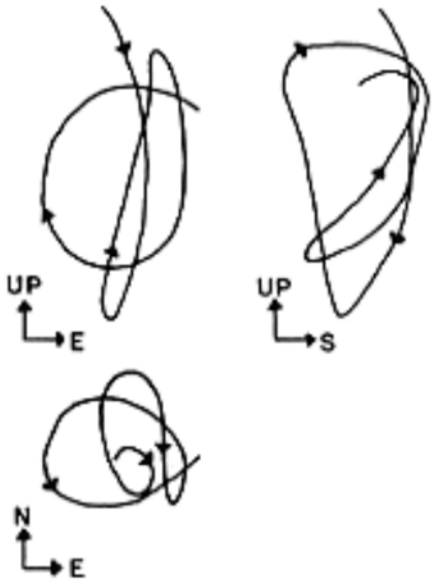

Figure 27.

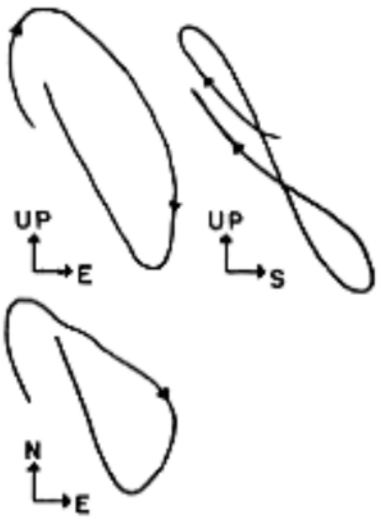

Figure 28a.

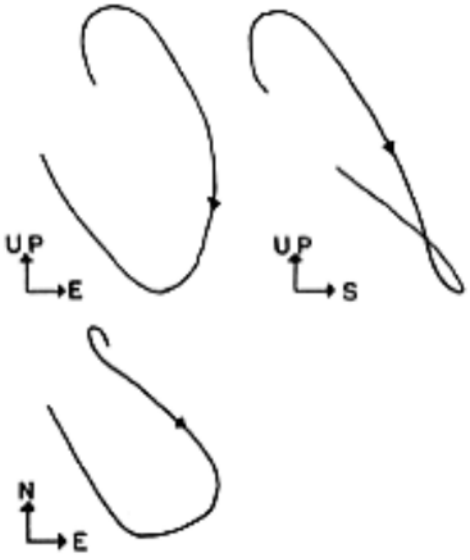

Figure 28b.

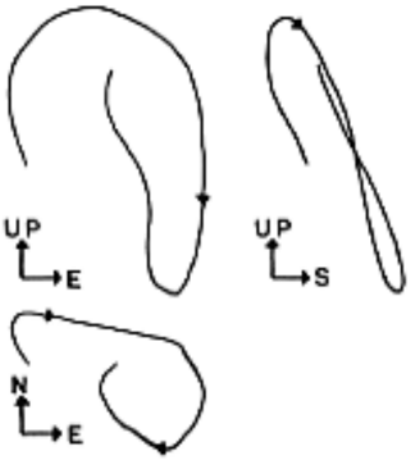

Figure 28c.

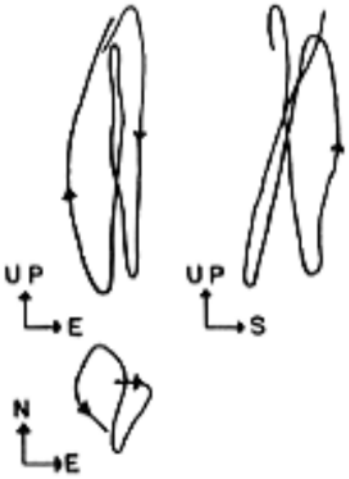

Figure 28d.

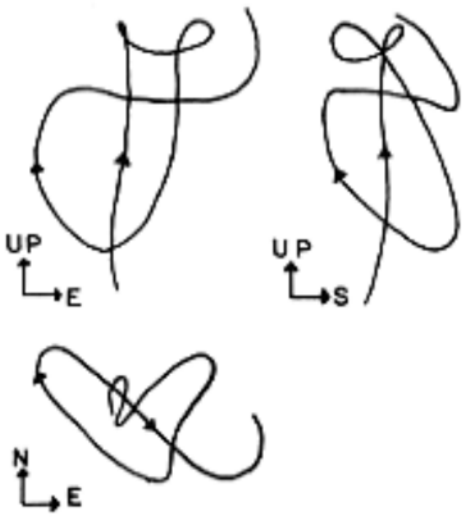

Figure 29.

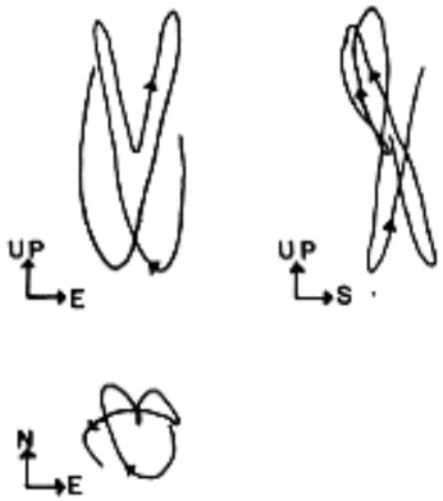

Figure 30.

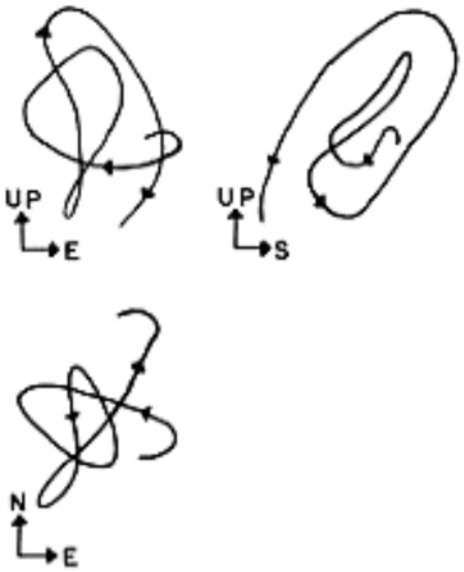

Figure 31.

Figure 32.

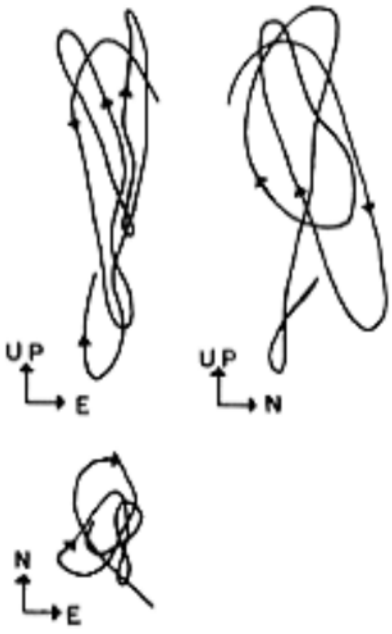

Figure 33a.

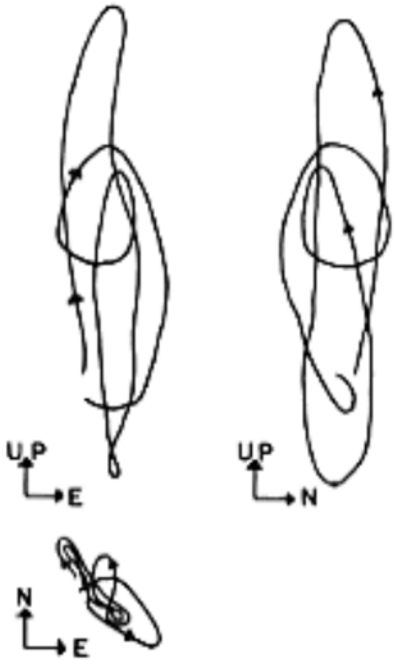

Figure 33b.

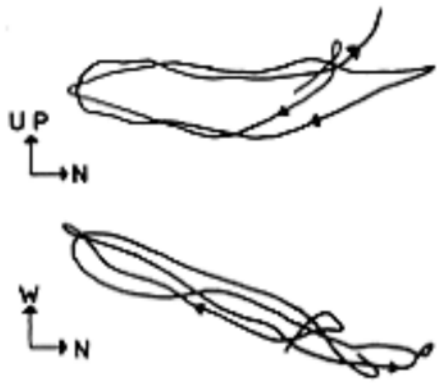

Figure 34a.

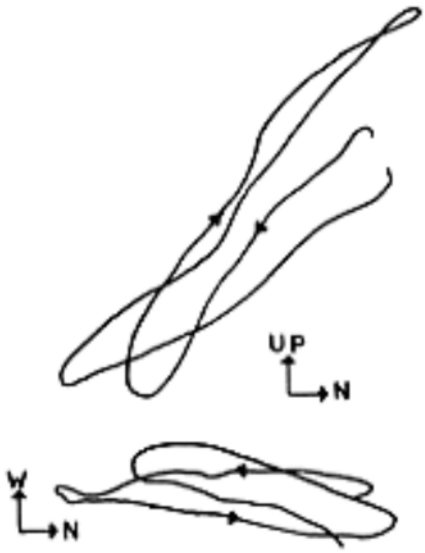

Figure 34b.

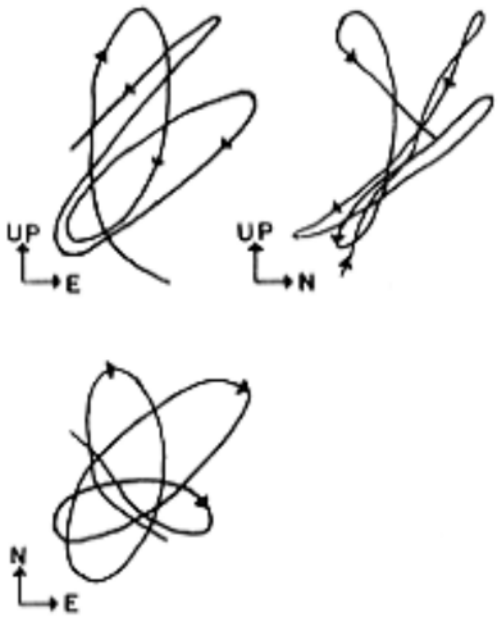

Figure 35.

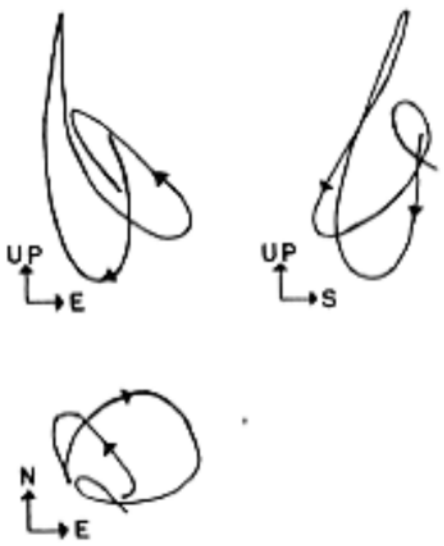

Figure 36.

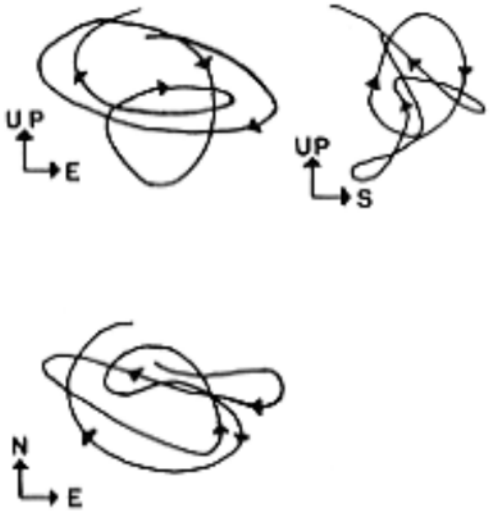

Figure 37.

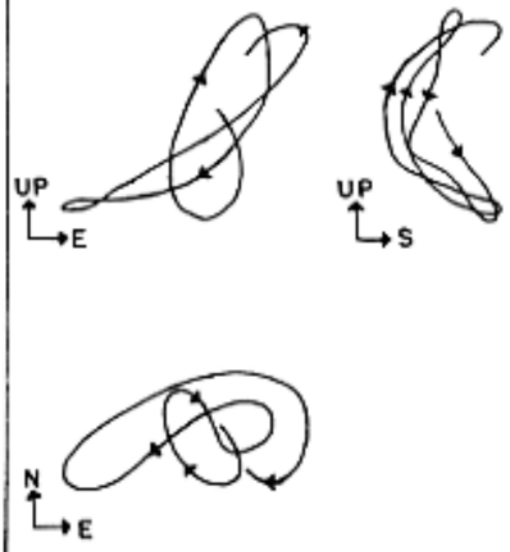

Figure 38.

Conclusions

At Socorro, microseisms in the frequency range of 2 to 5 cps are always present. They are generated by construction equipment, vehicular traffic, and trains. In this investigation, emphasis was placed on the train microseisms because their amplitudes are large and their point of origin is known. The position of the train was successfully determined between N-50-E and S-70-E from tripartite records of the train microseisms. Outside this zone, the increased topographic relief is sufficient to attenuate and scatter the microseisms seriously.

Peaks in number of determinations versus frequency were found at 2.9 and 3.4 cps. The interaction of surface waves of these two frequencies produces a beat effect found often on records of the train microseisms.

The measured phase velocities ranged from 1050 to greater than 2200 ft/sec. This spread can be explained by systematic errors in analysis, combination of waves from different directions, and interference by high-frequency (greater than 10 cps) microseisms. A peak in the distribution of velocity measurements at 1350 ft/sec corresponds to the measured phase velocity of Rayleigh waves having a mean frequency

of 2.9 cps.

Both Rayleigh and Love waves could be recognized in the particle motion figures. Many of the Rayleigh wave diagrams examined showed a tilt of the major axis of about 12 degrees in the direction of propagation and an axial ratio close to the theoretical value. In general, however, the particle motions were complex. This complexity can be explained by the combination of Love and Rayleigh waves of different frequency, phase, and direction of approach.

Suggestions for Further Investigation

(1) In particle motion studies the determination of wave type requires knoweldge of the direction of wave propagation. Additional instruments should be introduced into the network to enable three-component and tripartite recored to be taken simultaneously. With this arrangement it would be possible to determine the direction of approach for each particle motion.

(2) A strong dependece of the spread in direction determinations on topographic relief has been indicated. A study should be made to determine precisely what effect the topographic relief has on the propagation of short-period surface waves.

(3) The frequency analysis in this study has indicated two peaks. A more exact analysis should be made to determine if other smaller peaks in the frequency spectrum exist.

(4) A preliminary investigation of the wind noise on March 4, 1964, indicated that it contained microseisms in the frequency range of 2 to 5 cps. A study should be undertaken to determine to what extent microseisms in this frequency range are generated by strong surface winds.

References

Akamatu, Kei, (1961) On microseisms in frequency range from 1c/s to 200c/s, Bull. Earthquake Research Inst., Tokyo Univ., v. 39, pp. 23-75.

Ballenger, R. Lewis, (1963) Microseismic activity near Socorro, New Mexico, Unpublished report on file, New Mexico Institute of Mining and Technology.

Donn, W. L. and M. Blaik, (1953) A study and evaluation of the tripartite seismic method of locating hurricanes, Bull. Seism. Soc. Am., v. 43, pp. 311-329.

Eisler, J. D., (1952) Studies of a seismic surface disturbance, Geophysics, v. 17, pp. 550-559.

Ewing, M. W., W. S. Jardetzky, and F. Press, (1957) Elastic Waves in Layered Media, McGraw-Hill Book Co. Inc., New York.

Frantti, G. E., D. E. Willis, and J. J. Wilson, (1962) The spectrum of seismic noise, Bull. Seism. Soc. Am., v. 52, pp. 113-121.

Frantti, G. E., (1963) The nature of high-frequency earth noise spectra, Geophysics, v. 28, pp. 547-562.

Gutenberg, B., (1958) Two types of microseisms, Jour. Geophys. Res., v. 63, pp. 595-597.

Haskel, N. A., (1951) A note on air-coupled surface waves, Bull. Seism. Soc. Am., v. 41, pp. 295-300.

Heinrich, Rose R., Braught Gene, and F. K. Chang, (1957) Observations of ground vibrations in loess at Florissant, Missouri, Earthquake Notes, v. 28, pp. 16.

Kanai, Kiyoshi, T. Tanaka, and K. Osada, Measurement of micro-tremor I, to Measurement of micro-tremor VII, Bull. Earthquake Research Inst., Tokyo Univ.,

(1954) I v. 32, pp. 199-209.

(1957a) II v. 35, pp. 109-133.

(1957b) III v. 35, pp. 135-148.

(1957c) IV v. 35, pp. 149-162.

(1957d) V v. 35, pp. 163-180.

(1957e) VI v. 35, pp. 181-190.

(1957f) VII v. 35, pp. 191-200.

Kanai, Kiyoshi, and T. Tanaka, (1961) On micro-tremors VIII, Bull. Earthquake Research Inst., Tokyo Univ., v. 39, pp. 97-114.

Leet, L. D., (1949) Discussion of tripartite microseisms measurements, Bull. Seism. Soc. Am., v. 39, pp. 249-255.

Officer, C. B., (1958) Introduction to the Theory of Sound Transmission, McGraw-Hill Book Co. Inc., New York.

Ramirez, J. E., (1948) Short period microseisms, Trans., Am. Geophys. Un., v. 29, pp. 570-574.

Schuyler, G. L., (1955) Computations of the directions of microseisms at tripartite stations, Bull. Seism.

Soc. Am., v. 45, pp. 285-288

Walsh, D. H., (1955) An observational study of the origin of short-period microseisms near St. Louis, Missouri, Trans., Am. Geophys. Un., v. 45, pp. 285-288.

Wilson, C. D. V., (1953) The origin and nature of Microseisms in the frequency range 4 to 100 cyc/sec, Proc., Roy. Soc., v. A217, pp. 176-188.

Wilson, C. D. V., (1953) Analysis of the vibrations emitted by some man made sources of microseisms, Proc., Roy. Soc., v. A217, pp. 188-202.

Acknowledgements

The work presented in this thesis was performed under the direction of Dr. Allan R. Sanford of the New Mexico Institute of Mining and Technology. The author takes this opportunity to express his appreciation to Dr. Sanford for his assistance, guidance and helpful suggestions during the investigation. The assistance of Dr. Charles R. Holmes in the use of the instruments and the assistance of Mr. R. Ramanantoandro in the analysis of the data is gratefully acknowledged.

This thesis is accepted on behalf of the faculty of the Institute by the following committee:

Allan R. Sandage

Gerard Wolfgang Groh.

Ralph M. McGehee

Charles A Holmes

A. T. Bradding

Date: May 28, 1964